

Communication

Beyond the Active Site: Tuning the Activity and Selectivity of a Metal-Organic Framework-Supported Ni Catalyst for Ethylene Dimerization

Jian Liu, Jingyun Ye, Zhanyong Li, Ken-ichi Otake, Yijun Liao, Aaron W. Peters, Hyunho Noh, Donald G. Truhlar, Laura Gagliardi, Christopher J. Cramer, Omar K. Farha, and Joseph T. Hupp

J. Am. Chem. Soc., **Just Accepted Manuscript** • DOI: 10.1021/jacs.8b06006 • Publication Date (Web): 24 Aug 2018

Downloaded from <http://pubs.acs.org> on August 24, 2018

Just Accepted

“Just Accepted” manuscripts have been peer-reviewed and accepted for publication. They are posted online prior to technical editing, formatting for publication and author proofing. The American Chemical Society provides “Just Accepted” as a service to the research community to expedite the dissemination of scientific material as soon as possible after acceptance. “Just Accepted” manuscripts appear in full in PDF format accompanied by an HTML abstract. “Just Accepted” manuscripts have been fully peer reviewed, but should not be considered the official version of record. They are citable by the Digital Object Identifier (DOI®). “Just Accepted” is an optional service offered to authors. Therefore, the “Just Accepted” Web site may not include all articles that will be published in the journal. After a manuscript is technically edited and formatted, it will be removed from the “Just Accepted” Web site and published as an ASAP article. Note that technical editing may introduce minor changes to the manuscript text and/or graphics which could affect content, and all legal disclaimers and ethical guidelines that apply to the journal pertain. ACS cannot be held responsible for errors or consequences arising from the use of information contained in these “Just Accepted” manuscripts.

Beyond the Active Site: Tuning the Activity and Selectivity of a Metal–Organic Framework-Supported Ni Catalyst for Ethylene Dimerization

Jian Liu,^{†,⊥} Jingyun Ye,^{‡,⊥} Zhanyong Li,^{†,⊥} Ken-ichi Otake,[†] Yijun Liao,[†] Aaron W. Peters,[†] Hyunho Noh,[†] Donald G. Truhlar,[‡] Laura Gagliardi,[‡] Christopher J. Cramer,[‡] Omar K. Farha^{*,†,§,||} and Joseph T. Hupp^{*,†}

[†] Department of Chemistry, Northwestern University, 2145 Sheridan Road, Evanston, Illinois 60208, United States.

[‡] Department of Chemistry, Minnesota Supercomputing Institute, and Chemical Theory Center, University of Minnesota, Minneapolis, Minnesota 55455, United States.

[§] Department of Chemistry, Faculty of Science, King Abdulaziz University, Jeddah 21589, Saudi Arabia.

^{||} Department of Chemical and Biological Engineering, Northwestern University, 2145 Sheridan Road, Evanston, Illinois 60208, United States.

Supporting Information Placeholder

ABSTRACT: To modify its steric and electronic properties as a support for heterogeneous catalysts, electron-withdrawing and electron-donating ligands, hexafluoroacetylacetonate (Facac[−]) and acetylacetonate (Acac[−]), were introduced to the metal–organic framework (MOF), NU-1000, via a process akin to atomic layer deposition (ALD). In the absence of Facac[−] or Acac[−], NU-1000-supported, AIM-installed Ni(II) sites yield a mixture of C₄, C₆, C₈, and polymeric products in ethylene oligomerization. (AIM = ALD-like deposition in MOFs). In contrast, both Ni-Facac-AIM-NU-1000 and Ni-Acac-AIM-NU-1000 exhibit quantitative catalytic selectivity for C₄ species. Experimental findings are supported by density functional theory calculations, which show increases in the activation barrier for the C–C coupling step, due mainly to rearrangement of the siting of Facac[−] or Acac[−] to partially ligate added nickel. The results illustrate the important role of structure-tuning support modifiers in controlling the activity of MOF-sited heterogeneous catalysts and in engendering catalytic selectivity. The results also illustrate the ease with which crystallographically well-defined modifications of the catalyst support can be introduced when the node-coordinating molecular modifier is delivered via the vapor phase.

Heterogeneous catalysis is central to chemical and polymer manufacturing,¹ a variety of environmental remediation processes,² and many other chemo-centric endeavors.³ Appropriately chosen supports can be used to modulate the electronic properties of deposited active species, potentially yielding desirable changes in catalyst activity or chemical selectivity.^{4,5} Inorganic-oxides^{6–8} constitute a widely studied and broadly effective family of supports. Nevertheless, fine-tuning support properties using solely inorganic components can be challenging. We reasoned that metal-organic frameworks (MOFs), could function as both broadly and finely tunable heterogeneous-catalyst supports; here we present such results.

MOFs constitute a large and growing class of porous, crystalline materials.⁹ Broad tuning of MOF physical and chemical properties is achievable via modulation of metal-containing nodes

and/or the interconnecting organic linkers,¹⁰ making them promising materials for a broad range of potential applications, including gas separation,¹¹ gas storage and release,¹² chemical sensing,¹³ and heterogeneous catalysis.¹⁴ NU-1000, a MOF of *scu* topology featuring Zr₆(μ₃-O)₄(μ₃-OH)₄(H₂O)₄(OH)₄ clusters as nodes (abbreviated as Zr₆) and tetrapopic 1,3,6,8-(*p*-benzoate)pyrene (TBAPy^{4−}) units as linkers,¹⁵ has proven effective as a support for well-defined oxy-metal catalysts, including catalysts for ethylene hydrogenation and oligomerization,¹⁶ propane oxidative dehydrogenation,¹⁷ and alkene epoxidation.¹⁸

Work in our labs has shown that vapor-phase “AIM” (ALD-like chemistry in MOFs) is effective for assembling uniform arrays of catalytically active, metal-oxygen and metal-sulfur clusters directly on MOF nodes.^{16,18} For example, the material, Ni-AIM-NU-1000, exhibits high activity for ethylene oligomerization upon addition of the co-catalyst, (CH₃CH₂)₂AlCl. However, this catalyst generates a wide distribution of products, including C₄, C₆, and C₈, as well as undesirable polymeric material.^{16a}

Catalysts that selectively facilitate the production of C₄ (1-butene) from ethylene are of great interest since 1-butene is a widely used co-monomer in the commercial gas-phase synthesis of linear low-density polyethylene. We reasoned that appropriate tuning of the steric and electronic environment near the Ni(II) active site of Ni-AIM-NU-1000 might modulate its activity and/or catalytic chemical selectivity. As a starting point, and as a proof-of-concept, we first introduced highly electron-withdrawing or weakly electron-donating ligands for Zr₆, hexafluoroacetylacetonate (Facac[−]) or acetylacetonate (Acac[−]), followed by AIM installation of Ni(II); the resulting materials are termed Ni-Facac-AIM-NU-1000 and Ni-Acac-AIM-NU-1000, respectively (Figure 1). Notably, support-ligand installation was accomplished via volatilization, vapor-phase delivery of, and MOF-permeation by the conjugate acids, HFacac and HACac, concomitant with release of aqua and hydroxo ligands. The organic elaboration brought about distinct decreases in catalytic activity for ethylene oligomerization. Also seen, however, was a remarkable increase in product selectivity, *i.e.* exclusive formation of C₄ (butene), with an overwhelming preference for the isomer, 1-butene. Density

functional theory (DFT) modeling provides key insights into the mechanistic basis for high catalytic chemical selectivity.

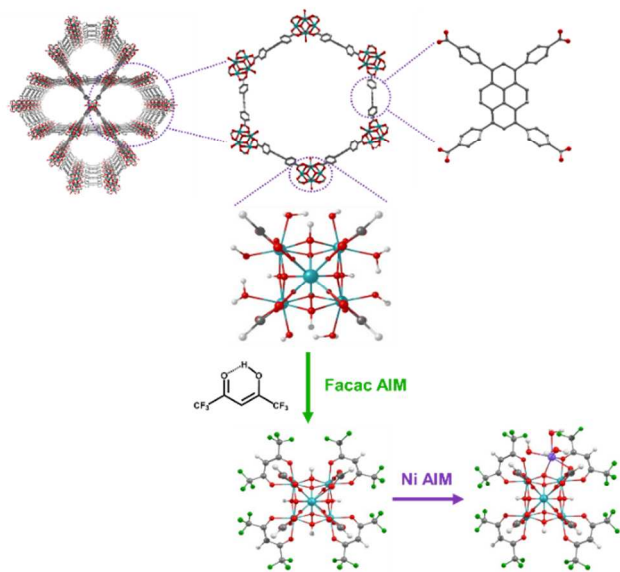


Figure 1. Schematic depiction of installation of the mono-anionic Facac^- ligand and Ni ions to the Zr_6 nodes of NU-1000. Color: C, grey; H, white; O, red; F, green; Ni, purple; Zr, cyan. (For clarity, linkers are truncated and shown as formate groups.) The indicated partial ligation of added Ni by Facac^- is derived from computations.

Due to the strong electron-withdrawing character of $-\text{CF}_3$ groups the single oxygen-bound proton is sufficiently acidic that ligation of Facac^- to MOF nodes via a process similar to solvent-assisted ligand incorporation (SALI)¹⁹ is expected. Because of the high vapor pressure of HFacac , Facac^- anions can be installed within NU-1000 via the molecular equivalent of ALD. Acac^- anions can be introduced in the same way. Acac^- incorporation can be quantified via ^1H spectroscopy, showing $\sim 2.8 \pm 0.1$ ligands per Zr_6 node before and after Ni AIM process. A combination of ^1H and ^{19}F NMR spectroscopy was used to quantify Facac^- incorporation, giving an average loading of $\sim 2.5 \pm 0.2$ ligands per Zr_6 node (Figure S1).

Diffuse reflectance infrared Fourier transform spectra suggest that the strength of binding of $-\text{OH}$ to nodes is altered by binding Acac^- or Facac^- to the nodes, as the $-\text{OH}$ stretching frequency shifts from 3674 to 3651 or 3642 cm^{-1} , respectively (Figure S2). One can imagine two possible modes of ligation for (F) acac^- : bridging between pairs of Zr(IV) ions or single-ligand chelation of one Zr(IV) . Single-crystal X-ray diffraction of the “molecular AIM” functionalized material revealed that each Facac^- anion chelates a single Zr ion (Figure S3 c & d) where the ligands point toward the hexagonal channels and toward pores perpendicular to the c -axis (Figures S3 a & b and Table S1).

Retention of $-\text{OH}$ stretches in the IR spectrum implies that Facac-AIM-NU-1000 and Acac-AIM-NU-1000 can be further functionalized with Ni(II). Using a procedure similar to that for Ni-AIM-NU-1000, the new materials, Ni-Facac-AIM-NU-1000 and Ni-Acac-AIM-NU-1000, were produced. The incorporation of Ni ions and retention of Facac^- ligands after the Ni-AIM were confirmed via X-ray photoelectron spectroscopy (XPS) (Figures S4 & S5). Important differences between the XPS spectra of NU-1000, Facac-AIM-NU-1000 , and Ni-Facac-AIM-NU-1000 are the inferred values of the $\text{Zr } 3d_{5/2}$ binding energy (Figure S4 a). Upon

coordination of Facac^- , the binding energy shifts from 182.9 to 183.3 eV; after Ni installation, it shifts slightly back to higher energy. These observations imply electronic communication between Facac^- ligands, Zr_6 nodes, and grafted Ni(II), behavior that was computationally probed by CM5 charge analysis.²⁰ (Table S2) The electronic effect of the more weakly electron-donating Acac^- ligands is not obvious in the XPS data. Detailed characterization (SEM/EDS, powder XRD and N_2 isotherms) of all samples indicated little difference in MOF crystallinity, particle morphology, or porosity (Figures S6–S8), thus underscoring the structural stability of the MOF with respect to node elaboration.

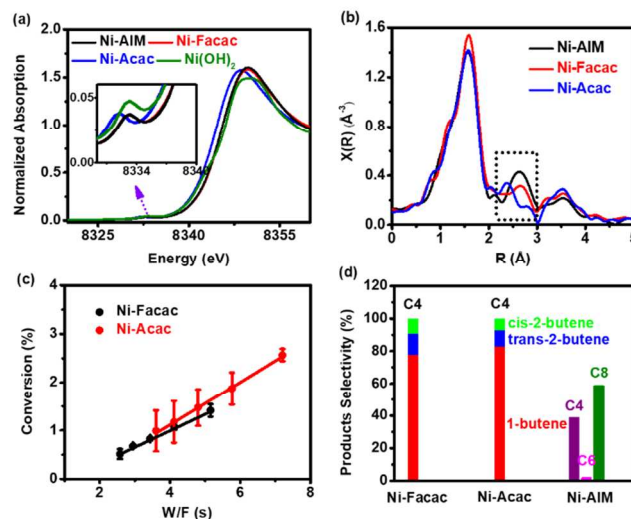


Figure 2. (a) X-ray absorption near-edge spectra (XANES) and (b) extended X-ray absorption fine structure spectra (EXAFS) for Ni-Facac-AIM-NU-1000, Ni-Acac-AIM-NU-1000 and Ni-AIM-NU-1000, and reference Ni(OH)_2 ; (c) conversion vs. W/F for ethylene dimerization catalyzed by activated Ni-Facac-AIM-NU-1000 and Ni-Acac-AIM-NU-1000; (d) product distribution for ethylene oligomerization as catalyzed by activated Ni-Facac-AIM-NU-1000 and Ni-Acac-AIM-NU-1000 compared to Ni-AIM-NU-1000. Note: data for Ni-AIM-NU-1000 are from reference 16a. (W=mol catalyst; F=flowrate reactant (mol/s))

X-ray absorption spectroscopy was employed to probe the valence and size of the Ni-oxo clusters in Ni-Facac-AIM-NU-1000 and Ni-Acac-AIM-NU-1000. Observable in the X-ray absorption near-edge spectral (XANES) region (Figure 2 a), is weak pre-edge peak corresponding to the $1s \rightarrow 3d$ transition at 8333.3 eV. This peak is indicative of divalent nickel, as observed in the Ni(II) standard (Ni(OH)_2) and in Ni-AIM-NU-1000. In the Fourier transformed extended X-ray absorption fine structure (EXAFS) spectrum, the dominant peak appears at a phase-uncorrected distance of ~ 1.62 Å; it can be fitted to a Ni–O scattering path featuring a bond length of 2.03 ± 0.01 and 2.05 ± 0.01 Å for Ni-Facac-AIM-NU-1000 and Ni-Acac-AIM-NU-1000, respectively. (Figures 2b, S9, S10, and S11 and Table S3.) The peak at 2.73 Å, which has been ascribed previously to Ni–Ni scattering,^{16a} is marginally weaker here than that in the EXAFS spectrum of Ni-AIM-NU-1000, implying a slightly smaller Ni-oxo cluster in the Facac/Acac-modified materials. This inference is in line with the results of inductively coupled plasma atomic emission spectroscopy (ICP-AES) results, which indicate Ni loadings of 3.4 ± 0.3 , 3.5 ± 0.4 and 4.0 ± 0.3 Ni/ Zr_6 for Ni-Facac-AIM-NU-1000, Ni-Acac-AIM-NU-1000 and Ni-AIM-NU-1000 to be, respectively.

To probe the effects of Acac^- and Facac^- ligands on the catalytic behavior of Ni-AIM-NU-1000, we examined the gas-phase oligomerization of ethylene. The three materials exhibit qualitatively similar catalytic behavior during the first 10 h time-on-stream (TOS), *viz.* (Figure S12a) modest decreases in catalytic activity presumably due to initial formation of polymeric products. C4 and C6 were also observed during the first 10 h TOS (Figure S12b). The turnover frequency (TOF) (on a per-nickel-atom basis) gradually decreases – ultimately stabilizing, after ~10 h, at $(3.5 \pm 0.78) \times 10^{-3} \text{ s}^{-1}$ for Ni-Facac-AIM-NU-1000 and $(4.4 \pm 0.85) \times 10^{-3} \text{ s}^{-1}$ for Ni-Acac-AIM-NU-1000 (Figure 2c), ~20 times lower than that for the modifier-free catalyst (0.07 s^{-1}).^{16a} Accompanying TOF stabilization is a refinement of the product distribution such that Ni-Facac-AIM-NU-1000 and Ni-Acac-AIM-NU-1000 both catalyze *only* C4 formation. In striking contrast, the unmodified catalyst even after several hours on stream, yields a mixture of C4, C6, and C8 products (Figure 2d). Characterization of the post-catalysis versions of Ni-Facac-AIM-NU-1000 and Ni-Acac-AIM-NU-1000 (Figures S13–S16) reveals retention of the original microparticle morphology and crystallinity, and retention of post-synthetically installed $\text{Facac}^-/\text{Acac}^-$ and Ni(II).

To understand the greatly enhanced selectivity for C4 engendered by elaborating the hexa-zirconium node (itself catalytically inactive), a Gibbs free energy profile was computationally modeled based on the proposed Zr_6 node structure model (Figure S17). While this model employs a single Ni atom in lieu of a larger Ni-oxo cluster, it should permit qualitative exploration of the influence of the installed ligands. (Thus, previous computations have shown single Ni atoms to be a good model for Ni_4 clusters specifically for understanding the catalytic activity of non-elaborated Ni-AIM-NU-1000 for ethylene dimerization.²¹) As illustrated in Figure 3, the catalytic cycle starts with the activated species **1**, where the ethyl group binds to Ni(II) via a strong β -agostic interaction with one H of the CH_3 group.^{16a, 16b, 22} An incoming ethylene binds to **1** at Ni(II) leading to the formation of **2**, which is exergonic by 8.3 kcal/mol for Ni-Facac-AIM-NU-1000. With a 26.6 kcal/mol free energy of activation, ethylene inserts into the Ni–C bond to produce **3** via transition-state (TS) structure TS2–3. With a subsequent free energy of activation of 9.6 kcal/mol (TS3–4), 1-butene is produced via β -hydrogen elimination with the concomitant formation of a nickel hydride species. After 1-butene desorption, ethylene can react with the nickel hydride species to reform **1**. Alternatively, **3** can further react with another ethylene molecule to produce a more stable structure **6** (5.4 kcal/mol lower than **3** in free energy). However, the migratory insertion of ethylene into the Ni–C bond in **6** to produce Ni–hexyl species **7** requires going through transition structure TS6–7 with a 24.5 kcal/mol free energy of activation, which is 9.5 kcal/mol higher than that to produce 1-butene. Therefore, the production of 1-butene is more favorable than the chain growth process to make oligomeric products, in line with the experimental observation (*vide supra*); Ni-Acac-AIM-NU-1000 shows similar selectivity to Ni-Facac-AIM-NU-1000 for 1-butene production because the free energy of activation for Ni-hexyl production (23.2 kcal/mol) is 11.2 kcal/mol higher than that for 1-butene production (Table S4). Also noteworthy is the computation that the activation barrier for the first C–C coupling step of unmodified Ni-AIM-NU-1000 (**2**→**3**) (13.7 kcal/mol) is 12.9 kcal/mol lower than that for Ni-Facac-AIM-NU-1000, consistent with the higher activity for ethylene oligomerization observed for the former. The lower activity of Ni-Facac/Acac-AIM-NU-1000 for ethylene dimerization derives partly from stronger binding of substrate to Ni and partly from greater costs for structural deformation along C–C coupling reaction pathways, likely due to rearrangement of the siting of

(F) acac^- to partially ligate added nickel (Figures 1 and 3; data in Tables S5 and S6).

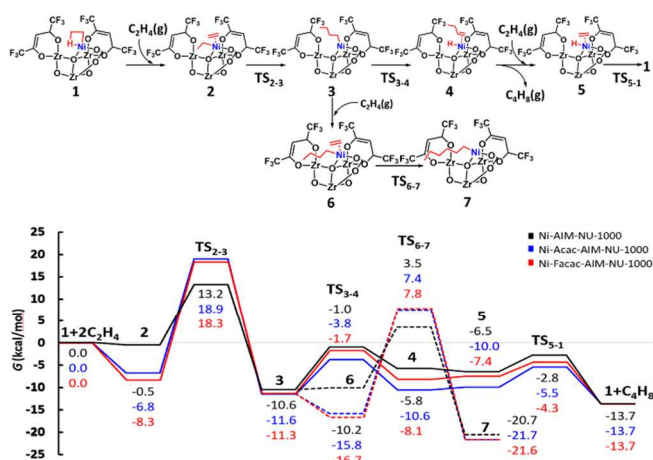


Figure 3. Gibbs free energy profiles (298.15 K, 1 atm) for the stationary points along reaction coordinates for ethylene oligomerization catalyzed by Ni-Acac-AIM-NU-1000 and Ni-Facac-AIM-NU-1000 compared to Ni-AIM-NU-1000.²² Solid and dash lines represent C2 to C4 and C4 to C6 reaction paths, respectively. Depictions of species in the catalytic cycle include only selected atoms for clarity.

In summary, molecular modifiers of MOF supports for heterogeneous catalysts can be introduced in atomically precise fashion via an ALD-like, vapor-phase delivery mechanism. For NU-1000, the modifiers Facac^- and Acac^- , displace node aqua and hydroxo ligands and bind to Zr(IV) in chelating fashion, as evidenced by single-crystal X-ray diffraction. Compared with the modifier-free catalyst (Ni-AIM-NU-1000), the new materials, Ni-Facac-AIM-NU-1000 and Ni-Acac-AIM-NU-1000, exhibit lower catalytic activity but remarkable changes in product selectivity for oligomerization of ethylene – most notably, *exclusive* formation of C4 (butene) species with a strong preference of the 1-butene isomer. DFT free energy profiles point to energetically more favorable butene release and diminished energetic access to a C–C bond forming, chain propagation step, when the support modifiers are present. The effects arise mainly from rearrangement of the siting of Facac^- or Acac^- and, therefore, partial ligation of added nickel (Figure 1). The strategy of automated, vapor-phase-mediated, modular assembly of uniform arrays of increasingly complex catalytic systems appears to provide a versatile way to fine-tune properties of the active-site, and to predictably define and control the chemical environment beyond the catalyst’s active site.

ASSOCIATED CONTENT

Supporting Information

The Supporting Information is available free of charge on the ACS Publications website. Materials synthesis, characterization data and computational details (PDF). X-ray crystallography for Facac-AIM-NU-1000 (CIF).

AUTHOR INFORMATION

Corresponding Authors

* O. K. F. (o-farha@northwestern.edu)
* J. T. H. (j-hupp@northwestern.edu)

Author Contributions

¹These authors contributed equally.

Notes

²The authors declare no competing financial interests.

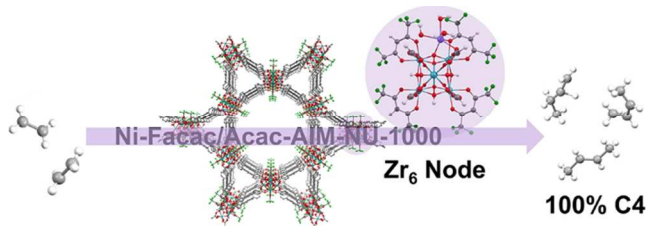
ACKNOWLEDGMENTS

³This work was supported as part of the Inorganometallic Catalyst Design Center, an EFRC funded by the DOE, Office of Science, Basic Energy Sciences (DE-SC0012702). H. N. gratefully acknowledges support from the Ryan Fellowship and the Northwestern University International Institute of Nanotechnology. This work made use of the J.B. Cohen X-ray Diffraction Facility supported by the MRSEC program of the National Science Foundation (DMR-1121262) at the Materials Research Center of Northwestern University. This work made use of the EPIC and Keck-II facilities of the NUANCE Center at Northwestern University, which has received support from the Soft and Hybrid Nanotechnology Experimental (SHyNE) Resource (NSF NNCI-1542205); the MRSEC program (NSF DMR-1121262) at the Materials Research Center; the International Institute for Nanotechnology (IIN); the Keck Foundation; and the State of Illinois, through the IIN. Use of the Advanced Photon Source is supported by the U.S. Department of Energy, Office of Science, and Office of Basic Energy Sciences, under Contract DE-AC02-06CH11357. Materials Research Collaborative Access Team (MRCAT, Sector10-BM) operations are supported by the Department of Energy and the MRCAT member institutions.

REFERENCES

- ⁴(1) Zaera, F. *Chem. Soc. Rev.* **2013**, *42*, 2746.
- ⁵(2) (a) Meng, X.; Wang, T.; Liu, L.; Ouyang, S.; Li, P.; Hu, H.; Kako, T.; Iwai, H.; Tanaka, A.; Ye, J. *Angew. Chem. Int. Ed.* **2014**, *53*, 11478. (b) Liu, J.; McCarthy, D. L.; Cowan, M. J.; Obuya, E. A.; DeCoste, J. B.; Skorenko, K. H.; Tong, L.; Boyer, S. M.; Bernier, W. E.; Jones, W. E. Jr. *Appl. Catal., B* **2016**, *187*, 154. (c) He, K.; Chen, G.; Zeng, G.; Chen, A.; Huang, Z.; Shi, J.; Huang, T.; Peng, M.; Hu, L. *Appl. Catal., B* **2018**, *228*, 19. (d) Ezzatahmedi, N.; Ayoko, G. A.; Millar, G. J.; Speight, R.; Yan, C.; Li, J.; Li, S.; Zhu, J.; Xi, Y. *Chem. Eng. J.* **2017**, *312*, 336.
- ⁶(3) Nie, Y.; Li, L.; Wei, Z. *Chem. Soc. Rev.* **2015**, *44*, 2168.
- ⁷(4) (a) Metzger, E. D.; Comito, R. J.; Hendon, C. H.; Dinca, M. *J. Am. Chem. Soc.* **2017**, *139*, 757. (b) Georgakilas, V.; Tiwari, J. N.; Kemp, K. C.; Perman, J. A.; Bourlinos, A. B.; Kim, K. S.; Zboril, R. *Chem. Rev.* **2016**, *116*, 5464.
- ⁸(5) (a) Yoshimaru, S.; Sadakiyo, M.; Staykov, A.; Kato, K.; Yamauchi, M. *Chem. Commun.* **2017**, *53*, 6720. (b) Wang, Y.; Widmann, D.; Behm, R. J. *ACS Catal.* **2017**, *7*, 2339.
- ⁹(6) Vilhanová, B.; Václavík, J.; Artiglia, L.; Ranocchiaro, M.; Togni, A.; van Bokhoven, J. A. *ACS Catal.* **2017**, *7*, 3414.
- ¹⁰(7) Ernst, J. B.; Muratsugu, S.; Wang, F.; Tada, M.; Glorius, F. *J. Am. Chem. Soc.* **2016**, *138*, 10718.
- ¹¹(8) Yilmaz, B.; Müller, U. *Top. in Catal.* **2009**, *52*, 888.
- ¹²(9) (a) Horike, S.; Shimomura, S.; Kitagawa, S. *Nat. Chem.* **2009**, *1*, 695. (b) Li, P.; Vermeulen, N. A.; Malliakas, C. D.; Gomez-Gualdron, D. A.; Howarth, A. J.; Mehdi, B. L.; Dohnalkova, A.; Browning, N. D.; O'Keeffe, M.; Farha, O. K. *Science* **2017**, *356*, 624. (c) Alezi, D.; Spanopoulos, I.; Tsangarakis, C.; Shkurenko, A.; Adil, K.; Belmabkhout, Y.; O'Keeffe, M.; Eddaoudi, M.; Trikalitis, P. N. *J. Am. Chem. Soc.* **2016**, *138*, 12767. (d) Yaghi, O. M. *J. Am. Chem. Soc.* **2016**, *138*, 15507. (e) Wang, C.; Liu, D.; Lin, W. *J. Am. Chem. Soc.* **2013**, *135*, 13222. (f) Zhou, H. C.; Long, J. R.; Yaghi, O. M. *Chem. Rev.* **2012**, *112*, 673. (g) Morris, W.; Voloskiy, B.; Demir, S.; Gandara, F.; McGrier, P. L.; Furukawa, H.; Cascio, D.; Stoddart, J. F.; Yaghi, O. M. *Inorg. Chem.* **2012**, *51*, 6443. (h) Feng, D.; Chung, W. C.; Wei, Z.; Gu, Z. Y.; Jiang, H. L.; Chen, Y. P.; Darensbourg, D. J.; Zhou, H. C. *J. Am. Chem. Soc.* **2013**, *135*, 17105.
- ¹³(10) (a) Zhou, T.; Du, Y.; Borgna, A.; Hong, J.; Wang, Y.; Han, J.; Zhang, W.; Xu, R. *Energy Environ. Sci.* **2013**, *6*, 3229. (b) Martell, J. D.; Porter-Zasada, L. B.; Forse, A. C.; Siegelman, R. L.; Gonzalez, M. I.; Oktawiec, J.; Runcevski, T.; Xu, J.; Srebro-Hooper, M.; Milner, P. J.; Colwell, K. A.; Autschbach, J.; Reimer, J. A.; Long, J. R. *J. Am. Chem. Soc.* **2017**, *139*, 16000. (c) Flaig, R. W.; Osborn Popp, T. M.; Fracaroli, A. M.; Kapustin, E. A.; Kalmutzki, M. J.; Altamimi, R. M.; Fathieh, F.; Reimer, J. A.; Yaghi, O. M. *J. Am. Chem. Soc.* **2017**, *139*, 12125.
- ¹⁴(11) Zhang, L.; Qian, G.; Liu, Z.; Cui, Q.; Wang, H.; Yao, H. *Sep. Purif. Technol.* **2015**, *156*, 472.
- ¹⁵(12) (a) Liao, Y.; Zhang, L.; Weston, M. H.; Morris, W.; Hupp, J. T.; Farha, O. K. *Chem. Commun.* **2017**, *53*, 9376. (b) Murray, L. J.; Dinca, M.; Long, J. R. *Chem. Soc. Rev.* **2009**, *38*, 1294. (c) Peng, Y.; Krungleviciute, V.; Eryazici, I.; Hupp, J. T.; Farha, O. K.; Yildirim, T. *J. Am. Chem. Soc.* **2013**, *135*, 11887.
- ¹⁶(13) Kreno, L. E.; Leong, K.; Farha, O. K.; Allendorf, M.; Van Duyne, R. P.; Hupp, J. T. *Chem. Rev.* **2012**, *112*, 1105.
- ¹⁷(14) (a) Lee, J.; Farha, O. K.; Roberts, J.; Scheidt, K. A.; Nguyen, S. T.; Hupp, J. T. *Chem. Soc. Rev.* **2009**, *38*, 1450. (b) Zhang, X.; Vermeulen, N. A.; Huang, Z.; Cui, Y.; Liu, J.; Krzyaniak, M. D.; Li, Z.; Noh, H.; Wasielewski, M. R.; Delferro, M.; Farha, O. K. *ACS Appl. Mater. Interfaces* **2018**, *10*, 635. (c) Bernales, V.; Ortuño, M. A.; Truhlar, D. G.; Cramer, C. J.; Gagliardi, L. *ACS Central Sci.* **2018**, *4*, 5.
- ¹⁸(15) Planas, N.; Mondloch, J. E.; Tussupbayev, S.; Borycz, J.; Gagliardi, L.; Hupp, J. T.; Farha, O. K.; Cramer, C. J. *J. Phys. Chem. Lett.* **2014**, *5*, 3716.
- ¹⁹(16) (a) Li, Z.; Schweitzer, N. M.; League, A. B.; Bernales, V.; Peters, A. W.; Getsoian, A. B.; Wang, T. C.; Miller, J. T.; Vjunov, A.; Fulton, J. L.; Lercher, J. A.; Cramer, C. J.; Gagliardi, L.; Hupp, J. T.; Farha, O. K. *J. Am. Chem. Soc.* **2016**, *138*, 1977. (b) Bernales, V.; League, A. B.; Li, Z.; Schweitzer, N. M.; Peters, A. W.; Carlson, R. K.; Hupp, J. T.; Cramer, C. J.; Farha, O. K.; Gagliardi, L. *J. Phys. Chem. C* **2016**, *120*, 23576. (c) Li, Z.; Peters, A. W.; Liu, J.; Zhang, X.; Schweitzer, N. M.; Hupp, J. T.; Farha, O. K. *Inorg. Chem. Front.* **2017**, *4*, 820.
- ²⁰(17) Li, Z.; Peters, A. W.; Platero-Prats, A. E.; Liu, J.; Kung, C.-W.; Noh, H.; DeStefano, M. R.; Schweitzer, N. M.; Chapman, K. W.; Hupp, J. T.; Farha, O. K. *J. Am. Chem. Soc.* **2017**, *139*, 15251.
- ²¹(18) Ahn, S.; Thornburg, N. E.; Li, Z.; Wang, T. C.; Gallington, L. C.; Chapman, K. W.; Notestein, J. M.; Hupp, J. T.; Farha, O. K. *Inorg. Chem.* **2016**, *55*, 11954.
- ²²(19) Deria, P.; Mondloch, J. E.; Tylianakis, E.; Ghosh, P.; Bury, W.; Snurr, R. Q.; Hupp, J. T.; Farha, O. K. *J. Am. Chem. Soc.* **2013**, *135*, 16801.
- ²³(20) Marenich, A. V.; Jerome, S. V.; Cramer, C. J.; Truhlar, D. G. *J. Chem. Theory Comput.* **2012**, *8*, 527.
- ²⁴(21) Ye, J.; Gagliardi, L.; Cramer, C. J.; Truhlar, D. G. *J. Catal.* **2017**, *354*, 278.
- ²⁵(22) Ye, J.; Gagliardi, L.; Cramer, C. J.; Truhlar, D. G. *J. Catal.* **2018**, *360*, 160.

1
2
3
4
5
6
7
8
9
10
11
12
13
14
15
16
17
18
19
20
21
22
23
24
25
26
27
28
29
30
31
32
33
34
35
36
37
38
39
40
41
42
43
44
45
46
47
48
49
50
51
52
53
54
55
56
57
58
59
60



TOC
